BAJOPMAS JOURNAL 16(1): 39 – 49
Printed in Bayero University, Kano - Nigeria.

EVALUATION OF CROSS-SECTIONS FOR NUCLEAR REACTIONS INVOLVING ALPHA PARTICLES: ISOTOPIC PRODUCTION OF BARIUM, LANTHANUM, AND CESIUM

[1]Ahmad, I.; [2]Ismaila, T., [3]Gambo, M. M. and [4]Abdulgadir, M.
[1] Department of physics, Bayero University Kano, Nigeria
[2,3]Departement of Applied Physics, School of Applied Sciences, Collage of Science and Technology, Kaduna Polytechnic, Kaduna, Nigeria
[4]Federal University of Transportation Daura, Katsina State, Nigeria
iahmad.phy@buk.edu.ng,Tijjaniismaila@Kadunapolytechnic.edu.ng,Mukhtarakad@gmail.com
Corresponding author: iahmad.phy@buk.edu.ng, +2348057303688

ABSTRACT
This study focuses on obtaining precise knowledge of reaction cross-sections and excitation function to enhance our understanding of nuclear interactions involving alpha particles. The cross-sections for producing isotopes of Barium, Lanthanum, and Cesium were evaluated using the EXIFON code. Notably, our findings indicate that the production of $^{132}Cs(a,3n)^{133}La$ is not observed within the energy range considered. Additionally, the reaction cross-sections, and excitation functions for the production of $^{136,135,134}La,\ ^{135,134}Ba, and\ ^{132,131,}Cs$, along with their respective threshold energies were obtained. These results contribute to a better understanding of nuclear processes involving alpha particles and the production of specific isotopes.

Keywords: Nuclear Reactions, Cross-Section, Alpha Particles, Isotopes, EXIFON code, Threshold Energies.

1.0 Introduction
Cesium has several important applications due to its unique physical properties, including its high atomic number and low melting point. One of its key applications is in atomic clocks, which are extremely accurate timekeeping devices that use the vibrations of cesium atoms to measure time [1]. Cesium is also utilized in radiography to inspect the integrity of pipelines, welds, and other industrial equipment [2][3]. In medicine, it plays a role in cancer treatment by delivering targeted radiation therapy. Additionally, cesium serves as a catalyst in chemical reactions, including the production of synthetic rubber and other polymers [5]. In glass production, cesium compounds enhance the clarity and durability of glass [6].

Cesium-132, however, is not a naturally occurring isotope; it is artificially produced through nuclear reactions. This radioactive isotope has a very short half-life of approximately three minutes and undergoes rapid decay, emitting high-energy beta and gamma particles. One method of producing cesium-132 involves irradiating stable cesium isotopes, such as cesium-133 or cesium-137, with neutrons in a nuclear reactor or with charged particles in a particle accelerator [7]. Due to its instability and short half-life, cesium-132 is not widely used in practical applications but is primarily of interest for nuclear reaction research and the study of radioactive isotopes [8].

The behavior of cesium-132 during particle interactions depends on the nature of the interaction. It undergoes rapid decay through the emission of high-energy particles, making it crucial to obtain more experimental cross-section data to better understand its nuclear interactions and decay processes. However, experimental data on the nuclear properties of cesium-132 remain limited. The nuclear cross-section, a fundamental parameter in nuclear reaction studies, determines the probability of a specific nuclear reaction occurring when an

incident particle interacts with a target nucleus. The cross-section varies based on the energy of the incident particle and the properties of the target nucleus, such as its mass and atomic number. [3,5].

Accurate cross-section data for cesium-132 is essential for modeling nuclear fuel behavior and understanding the effects of neutron irradiation on reactor materials. Additionally, such data is valuable for nuclear astrophysics, which examines the formation and evolution of stars and galaxies. Certain nuclear reactions involving cesium-132, such as neutron capture or beta decay, may contribute to the production or destruction of heavier elements in stars. Reliable cross-section data is crucial for accurately modeling these processes and understanding the chemical evolution of the universe. Furthermore, cesium-132 cross-section data is important for radiation dosimetry, which involves measuring and calculating radiation doses received by individuals or populations. This information helps estimate radiation exposure and its biological effects. [7,8].

While studies of nuclear reactions involving cesium-132 have primarily focused on its nuclear structure, decay modes, and cross-section data for reactions like neutron capture and beta decay, excitation function measurements could provide additional insights. These measurements would help determine the energy dependence of cesium-132 nuclear reactions, which is relevant for various applications in nuclear physics, nuclear energy, and astrophysics. [1,8].

In this study, the interaction cross-section of alpha particles with cesium-132 was calculated, and the excitation functions of elements produced through cesium-132 and alpha particle interactions were investigated within an energy range of 1–30 MeV. The threshold value, maximum cross-section, and energy corresponding to the maximum cross-section were identified.

2.0 Theoretical background

Statistical multistep reactions are also commonly used to describe nuclear reactions. In a nuclear reaction, a target nucleus is bombarded by a projectile, resulting in the formation of a compound nucleus. The compound nucleus then undergoes a series of reactions, leading to the emission of one or more particles or photons. In statistical multistep reactions, the formation and decay of the compound nucleus are treated as a series of elementary steps, each of which involves the absorption or emission of one or more particles or photons. The rate of each elementary step is determined by the thermodynamic properties of the system, such as the temperature and the level density of the states in the compound nucleus.

The overall rate of the nuclear reaction is determined by the rate of the slowest elementary step, which is usually the formation or decay of the compound nucleus. The other elementary steps are assumed to be in equilibrium, so that their rates can be calculated using statistical thermodynamics.

Statistical multistep reactions are widely used in nuclear physics to model a variety of nuclear processes, including nuclear fusion, fission, and spallation. They are also used in astrophysics to model the formation and evolution of stars and other astrophysical objects.
In the statistical multistep model, the total emission spectrum of the process (a,xb) is divided into three main part[9];[10],

$$\frac{\mathrm{d}\sigma_{\mathrm{a,xb}}(\mathrm{E_a})}{\mathrm{dE_b}} = \frac{\mathrm{d}\sigma_{\mathrm{a,b}}^{\mathrm{SMD}}(\mathrm{E_a})}{\mathrm{dE_b}} + \frac{\mathrm{d}\sigma_{\mathrm{a,b}}^{\mathrm{SMC}}(\mathrm{E_a})}{\mathrm{dE_b}} + \frac{\mathrm{d}\sigma_{\mathrm{a,xb}}^{\mathrm{MPE}}(\mathrm{E_a})}{\mathrm{dE_b}} \qquad (1)$$

The first term on the right hand side of Equation (1) represents the statistical multistep direct (SMD) part which contains from single-step up to five-step contributions. The second term

represents the statistical multistep compound (SMC) emission which is based on a master equation. Both terms together (SMD+SMC) represents the first-chance emission process. The last term of equation (1) represents the multiple particle emission (MPE) reaction which includes the second-chance, third-chance emissions, etc. These terms are summarized [11]:

$$\frac{d\sigma_{a,xb}^{MPE}(E_a)}{dE_b} = \sum_c \frac{d\sigma_{a,cb}(E_a)}{dE_b} + \sum_{c,d} \frac{d\sigma_{a,cdb}(E_a)}{dE_b} + \cdots \quad (2)$$

Activation Cross-sections

The following relations between the optical model (OM) reaction Cross-section and the energy-integrated partial Cross-sections should be satisfied (at each incident energy (E_a)) [11]

$$\sigma_a^{OM} = \sum_b \sigma_{a,b} \quad (3)$$

$$\sigma_{a,b} = \sum_c \sigma_{a,cb} \quad \text{and } \sigma_{a,cb} = \sum_d \sigma_{a,cdb} \quad (4)$$

with $\sigma_{a,b} = \sigma_{a,b}^{SMD} + \sigma_{a,b}^{SMC}$ the total first-chance emission, in this context, activation Cross-sections are given by;

$$\sigma_{a,b\gamma} = \sigma_{a,b} - \sum_{c\neq\gamma} \sigma_{a,cb} \quad (5)$$

$$\sigma_{a,cb\gamma} = \sigma_{a,cb} - \sum_{d\neq\gamma} \sigma_{a,cbd} \quad (6)$$

where $b, c, d \neq \gamma$

For example, the (n,p)-activation Cross-sections have the form

$$\sigma_{a,p\gamma} = \sigma_{n,p} - \sigma_{n,pn} - \sigma_{n,2p} - \sigma_{n,p\alpha} \quad (7)$$

The SMD Cross-section is a sum over s-step direct processes given by[12] :

$$\frac{d\sigma_{a,b}^{SMD}(E_a)}{dE_b} = \sum_{s=1} \frac{d\sigma_{a,b}^{s}(E_a)}{dE_b} \quad (8)$$

The SMD Cross-section has the form

$$\frac{d\sigma_{a,b}^{SMC}(E_a)}{dE_b} = \sigma_a^{SMC}(E_a) \sum\nolimits_{N=N_0}^{N^I} \frac{\tau_N(E)}{\hbar} \sum_{(\Delta V)} \Gamma_{N,b}^{(\Delta V)}(E, E_b) \uparrow \cdots \quad (9)$$

where τ_N satisfies the time-integrated master equation

$$-\hbar\delta_{NN_0} = \Gamma_{N-2}^{(+)}(E) \downarrow \tau_{N-2}(E) + \Gamma_{N+2}^{(-)}(E) \downarrow \tau_{N+2}(E) - \Gamma_N(E)\tau_N(E) \quad (10)$$

and

$$\Gamma_N^{(\Delta v)}(E) \downarrow = 2\pi I_{SS}^2 \rho_N^{(\Delta v)}(E) \quad (11)$$

The multiple particle emission is expressed as:

$$\frac{d\sigma_{a,xb}^{MPE}(E_a)}{dE_b} = \sum_c \frac{d\sigma_{a,cb}(E_a)}{dE_b} + \sum_{cd} \frac{d\sigma_{a,cdb}(E_a)}{dE_b} + \cdots \quad (12)$$

To keep the model tractable, a simple two-body interaction is assumed:[11]

$$I(r_1, r_2) = -4\pi \frac{F_0}{A} \left[\chi_{nl}(R)\right]^{-4} \delta(r_1 - r_2)\delta(r_1 - R) \quad (13)$$

$F_0 = 27.5$ MeV taken from nuclear structure considerations[13].

The factor $\left[\chi_{nl}(R)\right]^{-4}$ contains the wave function at the nuclear radius $R = r_0 A^{1/3}$

The single-particle state density of particles $C = n, p, \alpha$ with mass μ_c is given by [10];

$$\rho(E_c) = \frac{4\pi V \mu_c \left(2\mu_c E_c\right)^{1/2}}{(2\pi\hbar)}$$
$$= \left(4.48 \times 10^{-3} \mathrm{fm}^{-3} \mathrm{MeV}^{-3/2}\right) r_0{}^3 A E_C^{1/2} \quad (14)$$

where $V = \frac{4\pi R^3}{3}$ is equal to the nuclear volume.

The single-particle state density of bound particles (at Fermi energy) is then defined by

$$g = 4\rho(E_F) \quad (15)$$

where the factor 4 considers the spin and isospin degeneracy

3.0 Methodology

The EXIFON code is a nuclear reaction software that provides a continuous and smooth description of nuclear reactions over a wide energy and mass range. It is based on an analytical model for statistical multistep direct and multistep compound reactions (SMD/SMC model) [14]. This model predicts emission spectra, angular distributions, and activation cross-sections for neutrons, protons, alpha particles, and photons [10]. The calculations rely on random matrix physics using the Green's function formalism [15][16]. All calculations were performed without any free parameters, and results were generated for bombarding energies below 30 MeV [17][18].

Theoretical calculations of cross-sections were conducted using the EXIFON nuclear model code. The program was executed by defining the input and output directories, specifying the target nucleus, and selecting the incident particle and excitation function in the general options section. The number of incident energies was set to be zero (0) MeV, starting from a specified initial value with a defined energy step of 2 MeV. The cross-section corresponding to each particular energy was obtained.

3.0 Data Analysis

The computed cross-section values obtained from EXIFON were systematically analyzed to identify trends in reaction probabilities across different energy levels using Microsoft Excell. The output data (OUTEXI) files generated by EXIFON were stored in the designated output directory, along with DAT files for further processing. These data were visualized using graphical representations to observe the variation in cross-section values as a function of energy. The threshold energy for each reaction channel was identified and recorded, and dominant reaction mechanisms were determined by comparing neutron, proton, and alpha-particle emission cross sections. Additionally, the results were evaluated against existing experimental data to assess the accuracy of the EXIFON model predictions.

4.0 Results and Discursions

The results of the calculated cross-section as a function of energy are given in the tables. Graphs of the cross section against energy were plotted as shown in Figures 1 to 4.

Table 1. Calculated interaction cross section of alpha particle with cesium-132, and produce different type of reaction.

Energy (MeV)	Cross section Values (mb)														
	(a,a)	(a,na)	(a,ag)	(a,an)	(a,xa)	(a,g)	(a,ng)	(a,pg)	(a,2ng)	(a,xg)	(a,n)	(a,2n)	(a,pn)	(a,3n)	(a,xn)
1	0	0	0	0	0	0	0	0	0	0	0	0	0	0	0
2	0	0	0	0	0	0	0	0	0	0	0	0	0	0	0
3	0	0	0	0	0	0	0	0	0	0	0	0	0	0	0
4	0	0	0	0	0	0	0	0	0	0	0	0	0	0	0
5	0	0	0	0	0	0	0	0	0	0	0	0	0	0	0
6	0	0	0	0	0	0	0	0	0	0	0	0	0	0	0
7	0	0	0	0	0	0	0	0	0	0	0	0	0	0	0
8	0	0	0	0	0	0	0	0	0	0	0	0	0	0	0
9	0	0	0	0	0	0	0	0	0	0	0	0	0	0	0
10	0	0	0	0	0	0	0	0	0	0	0	0	0	0	0
11	0	0	0	0	0	0	0	0	0	0	0	0	0	0	0
12	0	0	0	0	0	0	0	0	0	0	0	0	0	0	0
13	0	0	0	0	0	3.5	5.4	0.9	0	9.8	5.4	0	0	0	5.4
14	0	0	0	0	0	8.9	44	6.4	0	59.3	44	0	0	0	44
15	0.3	0	0.3	0	0.3	9.4	104	14.7	0	128.4	104	0	0	0	104
16	1.1	0	1.1	0	1.1	8.6	181.9	25.2	0	216.9	181.9	0	0	0	181.9
17	3	0	3	0	3	7.9	276	38.1	0	324.9	276	0	0	0	276
18	6.1	0	6.1	0	6.1	7.2	385.7	53.5	0	452.5	385.7	0	0	0	385.7
19	9.4	0	9.4	0	9.4	6.5	497	69.5	0	582.4	497	0	0	0	497
20	13.8	0	13.8	0	13.8	5.7	594.8	84.3	0	698.6	594.8	0	0	0	594.8
21	18.4	0	18.4	0	18.4	5.1	678.8	94.8	0	797.1	681.6	0	3.3	0	684.9
22	22.7	0	22.7	0	22.7	4.5	702.5	91.4	22.4	843.4	759.2	22.4	19.4	0	801
23	26.6	0	26.6	0	26.6	4.1	596.5	77.3	126.3	830.6	828.9	126.3	45.2	0	1000.4
24	30	0	30	0	30	3.7	420.8	61.7	301.5	817.6	891.9	301.5	71.9	0	1265.4
25	33	0.1	32.4	0.5	33	3.4	270.6	46.2	467	819.5	949	467	98.2	0	1514.7
26	33.9	0.3	31.2	2.4	34.1	3.1	170.2	34.2	597.7	836.5	1002.3	597.7	120.7	0	1723
27	36.3	0.7	30.3	5.6	37.1	2.9	108.9	25.9	693.8	861.8	1049.3	693.8	139.1	0	1887.8
28	38.6	1.4	28.6	9.4	40.1	2.7	73.5	20.4	764.6	889.8	1092	764.6	154.3	0	2020.4
29	40.8	2.4	26.7	13.1	43.3	2.6	53.6	17	817.6	917.5	1131	817.6	167.1	0	2128.8
30	42.9	3.7	24.9	16.8	46.7	2.4	41.8	15.1	859.4	943.5	1166.4	859.4	178.2	0	2220.7

Table 1 presents cross-section values in millibarns, (mb) for various nuclear reactions involving cesium-132 as a function of incident alpha particle energy in MeV. Most reactions have a threshold energy above 10 MeV, meaning they do not occur at lower energies. Some reactions, such as (a,γ) and (a,p), start appearing around 13–15 MeV.

As the energy increases, the cross-section values generally increase, peaking at higher energies. The highest values are observed at 30 MeV, particularly for reactions like (a,2p) and (a,xn). The most dominant reactions at higher energies appear to be (a,p), (a,n), and (a,2n), which have significantly higher cross-section values compared to others.
The neutron-emitting channels (a,n, a,2n, etc.) tend to have higher cross-sections than proton or gamma emission channels at high energies. The presence of (a,2p) and (a,xn) at 30 MeV suggests complex reaction mechanisms involving multiple particle emissions.

The increasing cross-section at higher energies suggests that cesium-132 is more reactive under high-energy alpha bombardment. These values are crucial for nuclear reaction modeling, astrophysical studies, and radiation shielding calculations.

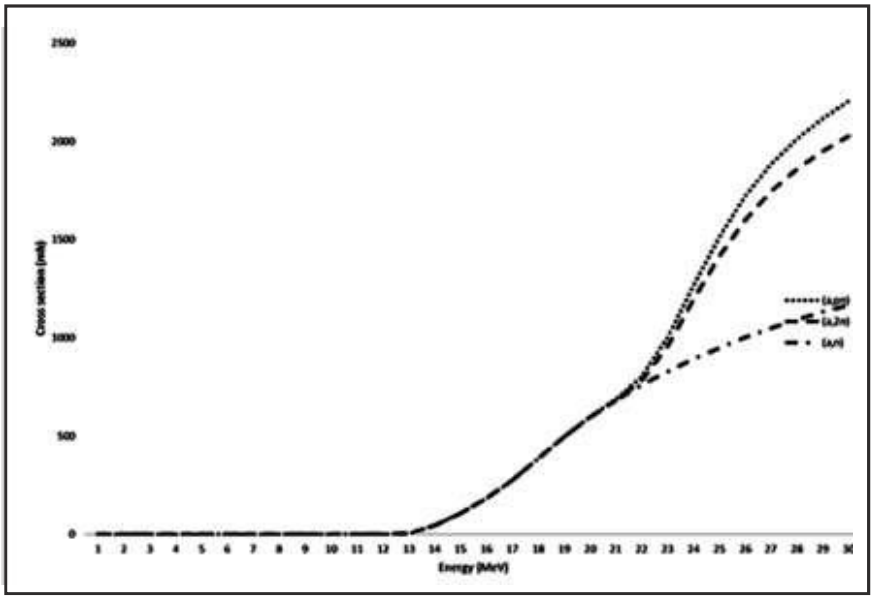

Figure 1. Cross-section vs energy of (a,pn), (a,2n) and (a,n) reactions

Figure 1 shows the cross-section reaction of :$^{132}Cs(a,n)^{135}La$ as the compound nuclear formation of lanthanum where by the incident alpha particle marge whith the nucleus of the cesium forming nucleus of ^{136}La isotope, later eject neutron from that nucleus. The reaction cross section increases with increase in energy at around 13 MeV, This shows that production of $^{135}\boldsymbol{La}$ through this route is possible at this energy range.

The Figure also shows that, the cross-section reaction of :$^{132}Cs(a,2n)^{134}La$ as the compound nuclear formation of lanthanum where by the incident alpha particle marge whith the nucleus of the cesium forming nucleus of ^{136}La isotope, which is later eject two neutrons from that nucleus. The reaction cross section increases with increase in energy at around 13 MeV, This shows that production of $^{134}\boldsymbol{La}$ through this route is possible at this energy range.

The Figure further shows the cross-section reaction of :$^{132}Cs(a,pn)^{134}Ba$ as the compound nuclear formation of Barium where by the incident alpha particle marge whith the nucleus of the cesium forming nucleus of ^{134}Ba isotope, then later eject a proton and one neutron from that nucleus. The reaction cross section increases with increase in energy at around 13 MeV, This shows that production of ^{134}Ba through this route is possible at this energy range.

From Table 1, It is observed that the cross-section reaction of :$^{132}Cs(a,3n)^{133}La$ as the compound nuclear formation of lanthanum were by the incident alpha particle marge with the nucleus of the cesium forming nucleus of ^{123}La isotope is not possible at the energy range provided. The reaction cross section is zero throughout the energy range, This shows that production of ^{133}La through this route is not possible at this energy range.

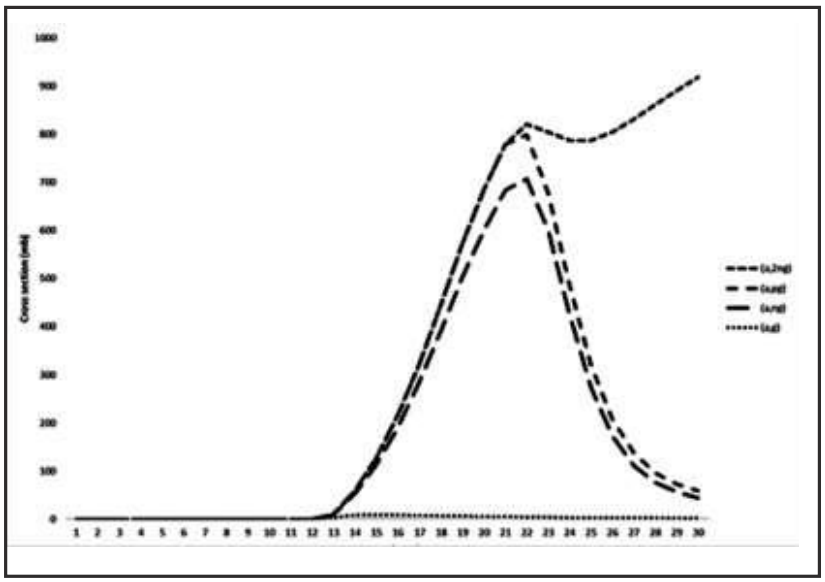

Figure 2. Cross-section vs energy of (a,2ng), (a,ng),(a,g) and (a,pg) reactions

Figure 2 shows the cross-section reaction of :$^{132}Cs(a,g)^{136}La$ as the compound nuclear formation of lanthanum where by the incident alpha particle marge whith the nucleus of the cesium forming nucleus of ^{136}La isotope. The gamma energy were ejected from the nucleus of lanthanum.The reaction cross section increases with increase in energy at around 13 MeV and it reaches maximum at energy around 15 MeV, the maximum cross section is about 9.4 mb This shows that production of ^{136}La through this route is possible at this energy range even though the cross section values is very small.

The Figure also shows the cross-section reaction of :$^{132}Cs(a,ng)^{135}La$ as the compound nuclear formation of lanthanum where by the incident alpha particle marge whith the nucleus of the cesium forming nucleus of ^{136}La isotope, later eject a neutron and gamma particles from that nucleus. The reaction cross section increases with increase in energy at around 13 MeV and it reaches maximum at energy around 22 MeV, the maximum cross section is about 702 mb, this shows that production of ^{135}La through this route is possible at this energy range.

The Figure further shows the cross-section reaction of: $^{132}Cs(a,pg)^{135}Ba$ as the compound nuclear formation of lanthanum where by the incident alpha particle marge whith the nucleus of the cesium forming nucleus of ^{136}La isotope, later eject a proton and gamma particles from that nucleus and produce ^{135}Ba. The reaction cross section increases with increase in energy at around 13 MeV, the maximum cross section is about 800 mb, this shows that production of ^{135}Ba through this route is possible at this energy range.

The Figure 2. Also shows the cross-section reaction of :$^{132}Cs(a,2ng)^{134}La$ as the compound nuclear formation of lanthanum where by the incident alpha particle marge whith the nucleus of the cesium forming nucleus of ^{134}La isotope, then later eject two neutrons and a gamma particles from that nucleus and produce ^{134}La. The reaction cross section increases with increase in energy at around 13 MeV, This shows that production of ^{134}La through this route is possible at this energy range.

Figure 3, Shows the cross-section reaction of :$^{132}Cs(a,a)^{132}Cs$ as the elastic collision where by the incident alpha particle interact elastically with the nucleus of the cesium. The reaction cross section increases with increase in energy at around 15 MeV, this is the threshold values of the reaction.

The Figure also shows the cross-section reaction of :$^{132}Cs(a,an)^{131}Cs$ as the pickup reaction where by the incident alpha particle removed a neutron from the nucleus of the cesium forming nucleus of ^{131}Cs isotope. The reaction cross section increases with increase in energy at around 16 MeV, This shows that production of ^{131}Cs through this route is possible at this energy range.

The Figure further shows the cross-section reaction of :$^{132}Cs(a,ag)^{132}Cs$ as the inelastic collision were by the incident alpha particle interact inelastically with the nucleus of the cesium. The nucleus of cesium was left at the excited state, later it decays through gamma emission. The reaction cross section increases with increase in energy at around 16 MeV. This is the threshold values of the reaction.

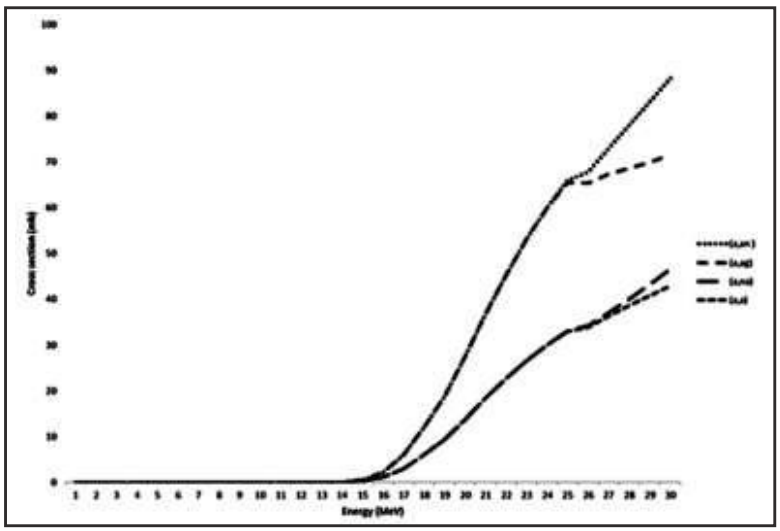

Figure 3. Cross-section vs energy of (a,an), (a,ag),(a,na) and (a,a) reactions

.The Figure 3. Also shows the cross-section reaction of $^{132}Cs(a,an)^{131}Cs$ as the pickup reaction were by the incident alpha particle interact with the nucleus of the cesium and removed a neutron from nucleus of ^{132}Cs□□ isotope. The reaction cross section increases with increase in energy at around 16 MeV, This shows that production of ^{131}Cs□□ through this route is possible at this energy range.

In Figure 4, the total cross-section reaction of (a,xa) where by the incident alpha particle interact whith the nucleus of the cesium forming nucleus of different channels that produce gamma particle. The reaction cross section increases with increase in energy at around 13 MeV and also shows the cross-section reaction of (a,xa) where by the incident alpha particle interact with the nucleus of the cesium forming nucleus of different channels that produce neutron.

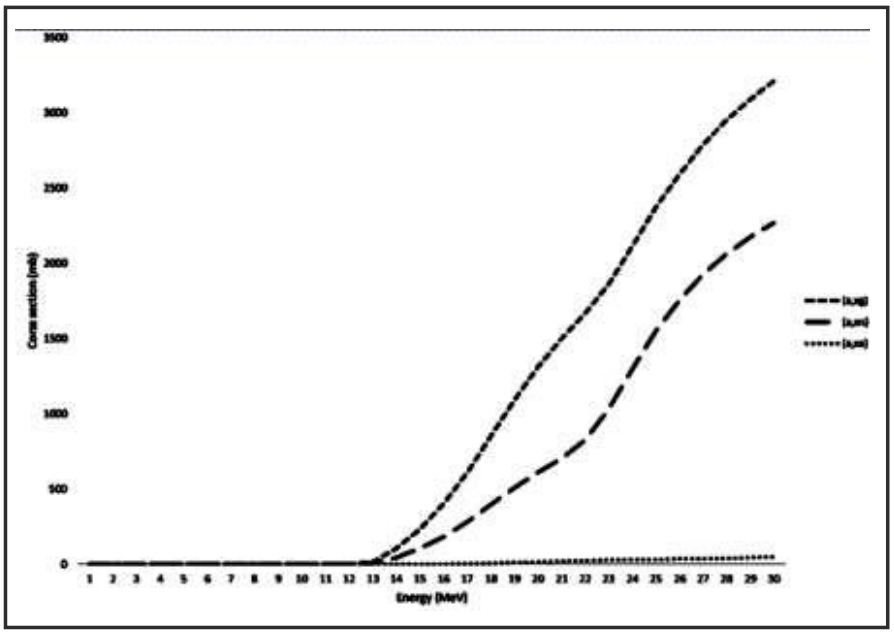

Figure 4. Cross-section vs energy of (a,xg), (a,xn), and (a,xa) reactions

The reaction cross section increases with increase in energy at around 14 MeV and also shows the cross-section reaction of (a,xa) where by the incident alpha particle interact whith the nucleus of the cesium forming different nucleus that produce alpha particle. The reactions that produce gamma particles have the highest cross section compared with the reactions that produce neutrons particles. The reaction that produced alpha particles have the lowest cross section compared with the gamma and neutrons producer.

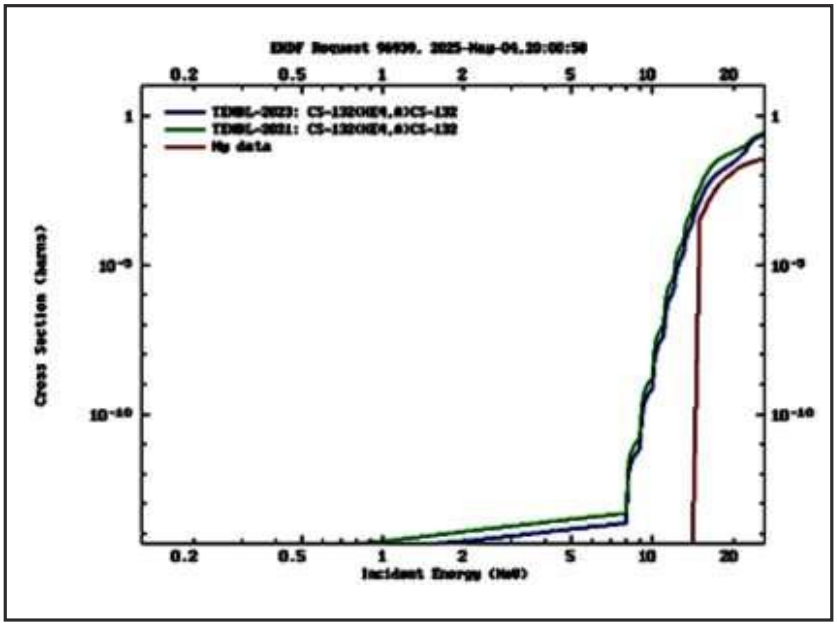

Figure 5. Cross-section vs energy of (a, a) reactions compares with other work at ENDF [19-20]

5. Conclusion

This study investigates the interaction of alpha particles with the radioactive isotope cesium-132 through theoretical modeling using the EXIFON code. The reaction cross-sections and corresponding excitation functions were calculated to determine the likelihood and energy dependence of various nuclear reaction channels.

A precise understanding of alpha-induced reaction cross-sections is critical for characterizing nuclear processes and improving predictive models in nuclear physics. In this work, Nuclear reactions were studied and the cross section for the production of isotopes of Barium, lanthanum and cesium were evaluated using EXIFON code. Our results show that production of $^{132}Cs(a,3n)^{133}La$ is not observed at considered energy range. The reaction cross section for the production of $^{136,135,134}La,\ ^{135,134}Ba, and\ ^{132,131,}Cs$ were obtained and their respective threshold energies. We also compare our results with others available evaluated nuclear data files to validate the results and are in good agreements.

References

[1] M. A. Lombardi, “The evolution of time measurement, part 3: Atomic clocks,” IEEE Instrum. Meas. Mag., vol. 14, no. 6, pp. 46–49, 2011, doi: 10.1109/MIM.2011.6086901.

[2] C. Woodford and P. Ashby, “Non-Destructive Testing and Radiation in Industry,” Aust. Inst. Non-Destructive Test., p. 3, 2001,. Available: https://www.osti.gov/etdeweb/servlets/purl/20267296

[3] X. F. Li, J. Sun, S. Lu, and L. Wang, “Application of On-line Digital Radiographic Inspection for Pipeline with Insulation,” J. Phys. Conf. Ser., vol. 2366, no. 1, 2022, doi: 10.1088/1742-6596/2366/1/012006.

[4] G. A. HAHN, “Radioisotopes in the treatment of pelvic cancer.,” Geriatrics, vol. 11, no. 3, pp. 113–118, 1956.

[5] L. F. Bobadilla et al., “Development of Power-to-X Catalytic Processes for CO2 Valorisation: From the Molecular Level to the Reactor Architecture,” Chem., vol. 4, no. 4, pp. 1250–1280, 2022, doi: 10.3390/chemistry4040083.

[6] N. H. Hamodi, T. J. Abram, T. Lowe, R. J. Cernik, and E. López-Honorato, “The chemical durability of glass and graphite-glass composite doped with cesium oxide,” J. Nucl. Mater., vol. 432, no. 1–3, pp. 529–538, 2013, doi: 10.1016/j.jnucmat.2012.09.010.
[7] IAEA, “Cyclotron Produced Radionuclides: Principles and Practice,” Cyclotr. Prod. Radionuclides Princ. Pract., no. 465, p. 230, 2008.
[8] M. Komljenović, G. Tanasijević, N. Džunuzović, and J. L. Provis, “Immobilization of cesium with alkali-activated blast furnace slag,” J. Hazard. Mater., vol. 388, no. October 2019, 2020, doi: 10.1016/j.jhazmat.2019.121765.
[9] I. Ahmad, Y. Y. Ibrahim, and F. S. Koki, “Evaluation of Reaction Cross Section of Radionuclide by Particles Induced Nuclear Reactions Using EXIFON Code,” Boson J. Mod. Phys., vol. 3, no. 2, pp. 236–244, 2017.
[10] Y. E. C. B. F. Ebiwonjumi, “Determination of Nuclear Reaction Cross-sections for Neutron- Induced Reactions in Some Odd – A Nuclides,” vol. 32, pp. 55–69, 2014.
[11] H. Kalka, “Hadrons and Nuclei Statistical multistep reactions from 1 to 100 MeV,” zeitchrift fur, Phys. A, vol. 299, pp. 289–299, 1992.
[12] I. Ahmad and F. S. Koki, “Calculation of Reactions Cross Section for Neutron-Induced Reactions on ¹²⁷I Isotope,” Int. J. Med. Physics, Clin. Eng. Radiat. Oncol., vol. 06, no. 03, pp. 344–359, 2017, doi: 10.4236/ijmpcero.2017.63031.
[13] S. M. Qaim, “A study of (n,na) reaction cross section at 14.7 MeV,” NUCL. PHYS. A, vol. 458, no. 2, pp. 237–245, 1986.
[14] T. F. O. and I. A. Temitope Fumilayo Ojo and Idris Ahmad, “Evaluation of Excitation Function of Nuclear Data on Proton Induced Reactions on Iridium,” Eval. Excit. Funct. Nucl. Data Prot. Induc. React. Iridium, vol. 15, no. Transaction of the Nigerian Association of Mathematical Physics, pp. 113–120, 2021.
[15] K. Muhammed, M. Y. Onimisi, and S. A. Jonah, “Investigation of the Shell Effect on Neutron Induced Cross Section of Actinides,” J. Nucl. Part. Phys., vol. 1, no. 1, pp. 6–9, 2011, doi: 10.5923/j.jnpp.20110101.02.
[16] Y. Watanabe et al., “Nuclear Data Evaluations for JENDL High-Energy File,” Int. Conf. Nucl. data Sci. Technol., vol. 769, pp. 326–331, 2005.
[17] H. Ford, “Radiation Safety Information Computational Center Changes To The Rsicc Code And data collection,” lawrence livermore national laboratory, livermore,USA. pp. 1–13, 2012.
[18] J. E. White, J. B. Manneschmidt, S. Y. Finch, and J. K. Dickens, “Abstracts Of Computer Programs And Data Libraries Pertaining To Photon Production Data,” Off. Sci. Tech. Inf. Tech. reports, vol. 32, pp. 101–103, 1997.
[19] A.J. Koning, D. Rochman, J.-Ch. Sublet, N. Dzysiuk, M. Fleming, and S. van der Marck, TENDL: Complete nuclear data library for innovative nuclear science and technology, Nuclear Data Sheets 155, 1 , 2019.
[20] R.E. Macfarlane and A.C. Kahler, Methods for processing ENDF/B-VII with NJOY, Nuclear Data Sheets 111, 2739 , 2010.